Original Research Article

Study of the impact of the magnetic field on the electrical parameters of the radial junction photovoltaic cell under monochromatic illumination.

Abstract

The present work is a theoretical study of the radial junction photovoltaic cell subjected to a magnetic field under monochromatic illumination. From a three-dimensional description, new analytical expressions of photocurrent density, photovoltage and electric power as a function of the magnetic field are established and by simulation on the Mathcad 15 software, we extracted the different curves. These representations allowed a thorough investigation of the operation of this model of a photovoltaic cell. It appears from this study that the amplitudes of parameters such as photocurrent density, photovoltage and electrical power are strongly attenuated when the photovoltaic cell is in the presence of a magnetic field assumed to be uniform over the entire region.

Keywords: Radial junction; magnetic field; photocurrent; photovoltage; electric power; monochromatic illumination

1 Introduction

The concept of the radial junction cell with a material such as silicon aims to reduce manufacturing costs and increase efficiency at the same time. To better understand the behaviour of such a cell,

our study will be carried out in the presence of a uniform magnetic field. Indeed, several authors have conducted similar studies to determine the influence of the tilt angle, such as Sahin [1] on a parallelepiped cell with a vertical junction, Sourabi [2] on a bifacial cell and Oudraogo [3] on the influence of a radio wave on a parallelepiped photovoltaic cell. Indeed, this geometry of the photovoltaic cell favours the absorption of almost all the incident light above the band [4] [5] due to its radial junction. To this end, we will first present the theories followed by the equations of our cell model and the boundary conditions established. We will then turn to the results and discussions and end with a summary of this study in the conclusion.

2 Theories

2.1 Model and theories.

We consider an elementary cell with a cylindrical silicon shape consisting of a P-doped base formed by an inner cylinder of radius R and an N+ doped emitter constituting the outer cylinder of radius R + d [6]. The intersection between the two cylinders represents the junction. The monochromatic illumination is done through the front face.

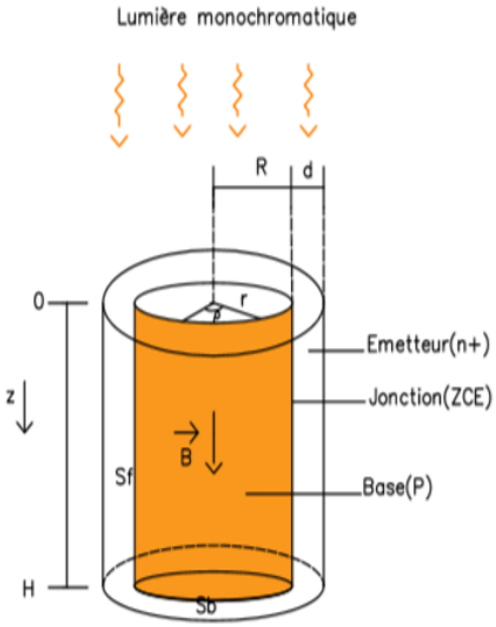

Figure 1: Photocurrent density as a function of the wavelength for different values of the magnetic field ($D_n = 26\text{cm}^2$; $Sb = 10^2\text{cm.s}^{-1}$; $L_n = R = 50\mu m$; $H = 100\mu m$).

2.2 Continuity equation

The magneto-transport equation which takes into account the magnetic field is given by the following equation:

$$\overrightarrow{j_n} = eD_n\overrightarrow{\nabla\delta} - \mu_n\overrightarrow{j_n} \wedge \overrightarrow{B} + e\mu_n\delta\overrightarrow{E} \tag{2.1}$$

$eD_n\overrightarrow{\nabla\delta}$: diffusion current
$\mu_n\overrightarrow{j_n} \wedge \overrightarrow{B}$: the current induced by the application of the magnetic field
$e\mu_n\delta\overrightarrow{E}$: conduction current

The continuity equation established through the magneto-transport equation is given by the following relation:

$$\frac{\partial^2\delta(r,z,\lambda)}{\partial r^2}+\frac{1}{r}\frac{\partial\delta(r,z,\lambda)}{\partial r}+\frac{1+(\mu_nB_0)^2}{1+\mu_nB_0}\frac{\partial^2\delta(r,z,\lambda)}{\partial z^2}-\frac{1+(\mu_nB_0)^2}{1+\mu_nB_0}\frac{\delta(r,z,\lambda)}{D_n\tau}=-\frac{1+(\mu_nB_0)^2}{1+\mu_nB_0}\frac{G(z,\lambda)}{D_n} \tag{2.2}$$

$G(z,\lambda)=\alpha(\lambda).\left[1-{R_n}'(\lambda)\right].\phi_0.e^{-\alpha(\lambda)z}$ is the electron generation rate
$\alpha(\lambda)$: the absorption coefficient as a function of wavelength
${R_n}'(\lambda)$: the monochromatic reflection coefficient of the material (polycrystalline silicon)

2.3 Density of electrons in the base

The solution to the continuity equation is as:

$$\delta(r,z,\lambda)=\sum_{k\geq 0}\left(A_k(\lambda)I_0\left(\frac{r}{{L_{nk}}^*}\right)+M_k(\lambda)\right)\sin\left(\frac{C_k}{\sqrt{\frac{1+(\mu_nB_0)^2}{1+\mu_nB_0}}}.z\right) \tag{2.3}$$

C_k reflects the concentration of charge carriers in the base. A_k et M_k are constants that are determined through the following boundary conditions:

- At the front

$$\delta(r,z=0,\lambda)=0 \tag{2.4}$$

- At the Transmitter-Base junction

$$\left.\frac{\partial\delta(r,z,\lambda)}{\partial r}\right|_{r=R}=-\frac{Sf}{2{D_n}^*}\delta(r=R,z,\lambda) \tag{2.5}$$

- On the rear side

$$\left.\frac{\partial\delta(r,z,\lambda)}{\partial z}\right|_{z=H}=-\frac{Sb}{{D_n}^*}\delta(r,z=H,\lambda) \tag{2.6}$$

2.4 Photocurrent density

The expression for the photocurrent density is given by the following relationship:

$$J_{ph} = \frac{qD_n{}^*}{R} \int_0^H -\frac{Sf}{D_n{}^*} \delta(r = R, z, \lambda) dz \tag{2.7}$$

2.5 Photovoltage

The photovoltage of our photovoltaic cell model is obtained through the Boltzmann relation:

$$V_{ph} = V_T \ln \left[1 + 2\pi R \frac{Nb}{{n_i}^2} \int_0^H \frac{-2D^*}{Sf} \left. \frac{\partial \delta(r, z, \lambda)}{\partial r} \right|_{r=R} dz \right] \tag{2.8}$$

3 Results and discussions

3.1 Photocurrent density Jph

The curves in the figure above (Figure 2) show the photocurrent density profiles as a function of wavelength for different values of the magnetic field.

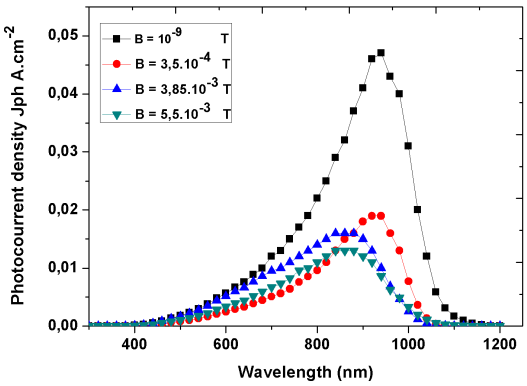

Figure 2: Photocurrent density as a function of the wavelength for different values of the magnetic field ($D_n = 26\text{cm}^2$; $Sb = 10^2\text{cm.s}^{-1}$; $L_n = R = 50\mu m$; $H = 100\mu m$).

From this representation, it is clear that the photocurrent density decreases as the magnetic field increases [7][8][9]. On the other hand, the curves show a shift of the maximum value of the

photocurrent corresponding to the wavelength for an almost zero magnetic field to the left, i.e. towards the low values of the wavelength, as the field increases. This study shows us that the magnetic field opposes the establishment of the photocurrent, hence the decrease in the curves. The shift of the photocurrent maximum to the left can be explained by the fact that the short wavelengths are absorbed in the surface with less recombination, whereas the generation of photocurrent at long wavelengths is attenuated by the presence of the magnetic field through the increase in recombination at depth. To further understand the behaviour of the photovoltaic cell, we will plot the profiles of the photocurrent density as a function of the dynamic junction velocity for the maximum wavelength. Following the representation of photocurrent density as a function of wavelength from which we have identified a maximum value of photocurrent density corresponding to the wavelength, we proceed to the representation of photocurrent density as a function of dynamic junction velocity for different values of the magnetic field.

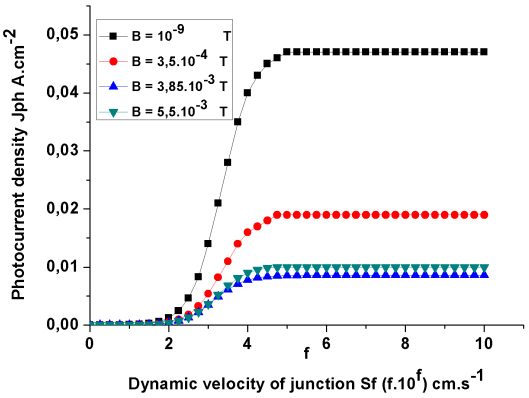

Figure 3: Photocurrent density as a function of dynamic velocity at the junction for different magnetic field values ($\lambda = 940\mu m$; $D_n = 26\text{cm}^2$; $Sb = 10^2\text{cm.s}^{-1}$; $L_n = R = 50\mu m$; $H = 100\mu m$).

We find a low photocurrent density in the open circuit situation, but the curves show constant curves in the short circuit [10]. Like the present observations, the magnetic field opposes the establishment of the photocurrent, generating more recombinations in proportion to the intensity of the magnetic field, hence a strong decrease in the photocurrent density. Indeed, a strong magnetic field tends to cancel the photocurrent even in a short-circuit situation.

3.2 Photovoltage Vph

The figure below (Figure 4) shows the photovoltage versus dynamic junction velocity curves for different magnetic field values.

In the open circuit situation, we have a high photovoltage in contrast to the short circuit where the photovoltage decreases sharply. Moreover, the curves show a decrease in photovoltage as the magnetic field intensity increases. This is because the magnetic field increases the recombination of charge carriers, which results in fewer stored carriers and therefore a decrease in photovoltage even in the open circuit situation.

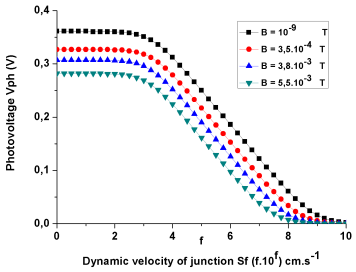

Figure 4: Photovoltage versus dynamic junction velocity for different magnetic field values ($\lambda = 940\mu m$; $D_n = 26\text{cm}^2$; $Sb = 10^2\text{cm.s}^{-1}$; $L_n = R = 50\mu m$; $H = 100\mu m$).

3.3 Electrical power Pl

The electrical power is the product of the photocurrent density generated and the photovoltage, whose relationship is as follows: $P_{el} = J_{ph}.V_{ph}$

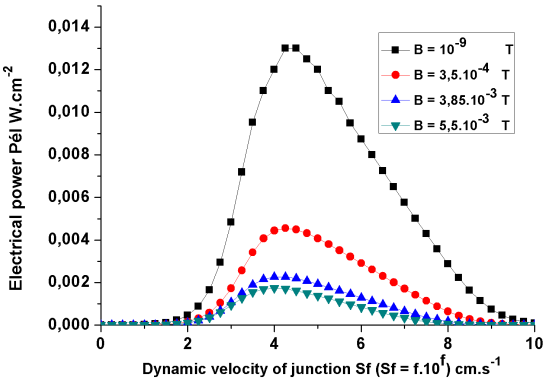

Figure 5: electrical power as a function of the dynamic velocity at the junction for different values of the magnetic field($D_n = 26\text{cm}^2$; $Sb = 10^2\text{cm.s}^{-1}$; $L_n = R = 50\mu m$; $H = 100\mu m$).

The electrical power is studied by representing its curves as a function of the dynamic junction speed for different magnetic field values. Firstly, we note parabolic profiles which can be explained by the fact that at low values of the dynamic junction velocity, the photocurrent is lower, but at short-circuit, the photovoltage is lower. As the electric power is the product of the voltage and the photocurrent, it is obvious that it decreases as the magnetic field intensity increases [11][12][13], which is in agreement with previous observations. In addition, the power maximum shifts towards the lower values of the dynamic junction velocity, which results in an increase in the load resistance and a reduction of the load current. In this section it is also shown that the magnetic field hurts

the performance of the radial junction photovoltaic cell by reducing the ability of the cell to generate current, resulting in a decrease in efficiency and form factor. This phenomenon leads to overheating of the cell due to strong recombinations, especially in volume and surface, which favours a rapid deterioration of the cell.
We continue the studies by evaluating the behaviour of the cell when given a radius, a scattering length, and the wavelength maintained at different values of the magnetic field. From this simulation, we have extracted the values of the electrical parameters parameterised by the electric field and recorded them in the table below (table 1).

Table 1: Electrical parameters of a radial junction photovoltaic cell for different magnetic field values.

$B(T)$	10^{-9}	$3{,}5.10^{-4}$	$3{,}85.10^{-3}$	$5{,}5.10^{-3}$
$V_{co}(V)$	0,360	0,327	0,307	0,282
$J_{cc}\left(mA.cm^{-2}\right)$	47,2	19,1	10,3	8,6
$V_{\max}(V)$	0,297	0,264	0,252	0,224
$J_{\max}\left(mA.cm^{-2}\right)$	42,9	17,3	9,0	7,7
$FF(\%)$	74,9	73,1	72,0	71,1

The values of the electrical parameters including Jcc, Jphmax, Vco, and Vmax are recorded in the table above (Table 1). The increase in the diffusion length leads to an increase in the values of the parameters. From this table, we can see that the form factor (FF) is close to the ideal as the diffusion length tends towards the radius of the base of the photovoltaic cell. The cell model studied has a geometry that is favourable to increasing the efficiency parameters because it allows the reduction of the number of materials to be reconciled with the electrical conversion efficiency. To achieve good efficiency, the diffusion length must be close to the radius of the base of the photovoltaic cell. Thus, the electrons will recombine closer to the junction which causes more photocurrent generation. In addition, the increase in photovoltage reveals that the carriers are more resistant to the major trap centres, which are partly responsible for the recombinations, leading to a decrease in surface and volume recombinations, which essentially contributes to the decrease in photovoltage.

4 CONCLUSIONS

Through three-dimensional modelling parameterised by the magnetic field, this study has allowed us to evaluate the impact of the magnetic field on the radial junction photovoltaic cell. In the present work, we have first presented the photovoltaic cell with the theories that accompany this work. Then, through the representation of the different curves obtained from a simulation on the Mathcad 15 software, we show the influence of the magnetic field on the radial junction photovoltaic cell. To show that this approach has many advantages due to the geometry of the cell which allows for improving the efficiency of the photocurrent generation while limiting the quantity of material used, reducing at the same time the production costs of photovoltaic systems on an industrial scale. However, photocells have potential limitations when exposed to a magnetic field, which is a factor opposing the establishment of the current.

References

[1] G.Sahin Effect of incidence angle on the electrical parameters of vertical parallel junction silicon solar cell under frequency domain, Moscow Univ. Phys. Bull., vol. 71, no. 5, pp. 498507, 2016, doi: 10.3103/S0027134916050088.

[2] I. Sourabi, 3D modeling of the effect of the intensity of an external magnetic field and its angle of incidence on the performance of a bifacial silicon photocell, 2018.

[3] A.Ouedraogo, 3D modeling of the influence of radio waves on a silicon photocell.

[4] M. D. Kelzenberg, M. C. Putnam, and N. S. Lewis, ," Oder, pp. 19481953, 2009.

[5] N. M. Ali, N. K. Allam, A. M. Abdel Haleem, and N. H. Rafat, Analytical modeling of the radial pn junction nanowire solar cells, J. Appl. Phys., vol. 116, no. 2, 2014, doi: 10.1063/1.4886596.

[6] a Trabelsi, a Zouari, and a Arab, Modeling of polycrystalline N/P junction solar cell with columnar cylindrical grain, Rev. des Energies Renouvelables VN - readcube.com, vol. 12, pp. 279297, 2009,

[7] M. L. Samb et al., 3-D modeling study of a silicon photocell in static mode placed in a magnetic and clearly multispectral field: determination of the electrical parameters., vol. 10, pp. 2338, 2010.

[8] M. I. Ngom et al., T Heoretical Study of a Parallel Vertical Multi- Junction Silicon Cell Under Multispectral Illumi- Nation: Influence of External Magnetic Field on, Int. J. Adv. Technol. Eng. Res., vol. 2, no. 6, pp. 101109, 2012.

[9] D. J. B. Issa Zerbo, Martial Zoungrana, Idrissa Sourabi, Adama Ouedraogo, Bernard Zouma, External Magnetic Field Effect on Bifacial Silicon Solar Cells Electrical Parameters, Energy Power Eng., vol. Vol.8 No.3, doi: 10.4236/epe.2016.83013.

[10] G. Sahin and G. Kerimli, Determination of the Junction Recombination Velocity Initiating the Short Circuit Situation Sfsc of a Bifacial Silicon Solar Cell Irradiated Under Magnetic Field in Dynamic Frequency Regime, Silicon, vol. 10, no. 4, pp. 16611665, 2018, doi: 10.1007/s12633-017-9650-x.

[11] I. Zerbo, M. Zoungrana, I. Sourabie, A. Ouedraogo, B. Zouma, and D. Joseph Bathiebo, External magnetic field effect on bifacial silicon solar cells electric power and conversion efficiency, Turkish J. Phys., vol. 39, no. 3, pp. 288294, 2015, doi: 10.3906/fiz-1505-10.

[12] D. U. Combari, I. Zerbo, M. Zoungrana, E. W. Ramde, and D. J. Bathiebo, Modelling Study of Magnetic Field Effect on the Performance of a Silicon Photovoltaic Module, Energy Power Eng., vol. 09, no. 08, pp. 419429, 2017, doi: 10.4236/epe.2017.98028.

[13] A. N. Dieng, N. Thiam, A. Thiam, S. Maiga, A, and G. Sissoko, Magnetic Field Effect on the Electrical Parameters of a Polycrystalline Silicon Solar Cell, Semicond. Sci. Technol., vol. 7, no. 3, pp. 602611, 2011, doi: 10.1088/0268-1242/26/9/095023.